A Prismatic Finite Element for Accurate Arch Dam Analysis

V. Mironov, Technische Universität Berlin, 13355 Berlin, Germany
(vadikmironoff@mtu-net.ru)
P.J. Pahl, Technische Universität Berlin, 13355 Berlin, Germany
(pahl@ifb.bv.tu-berlin.de)

Summary
The displacements and stresses in arch dams and their abutments are frequently determined with 20-node brick elements. The elements are distorted near the contact plane between the wall and the abutment. A cantilever beam testbed has been developed to investigate the consequences of this distortion. It is shown that the deterioration of the accuracy in the computed stresses is significant. A compatible 18-node wedge element with linear stress variation is developed as an alternative to the brick element. The shape of this element type is readily adapted to the shape of the contact plane. It is shown that the accuracy of the computed stresses in the vicinity of the contact plane is improved significantly by the use of wedge elements.

1 Development of a testbed for element behaviour
The reliable modelling and analysis of concrete arch dams has a significant influence on the evaluation of arch dam safety and usability. The linear and nonlinear behaviour of a specific dam must be investigated by static and dynamic finite element analyses considering the dam itself, its abutment and the reservoir. The precision of such analyses depends on the types of finite elements that are used in the structural model.

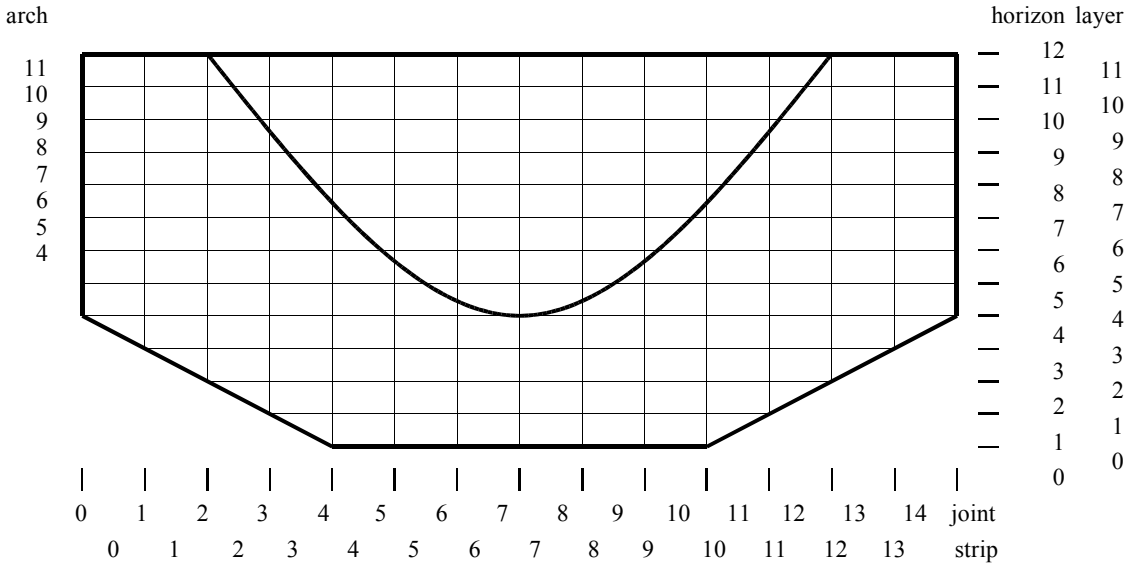

Fig. 1 : Elevation of the Arch Dam and Abutment

A finite element grid for an arch dam is shown in Fig. 1. The grid is generated so that the horizontal and vertical joints and the contact plane between the dam and the abutment coincide with surfaces of the finite elements. In the past, twenty node brick elements of the serendipity type shown in Fig. 2 have frequently been used for the finite element analysis of arch dams (Zienkiewicz 1977), (Bathe 1986).

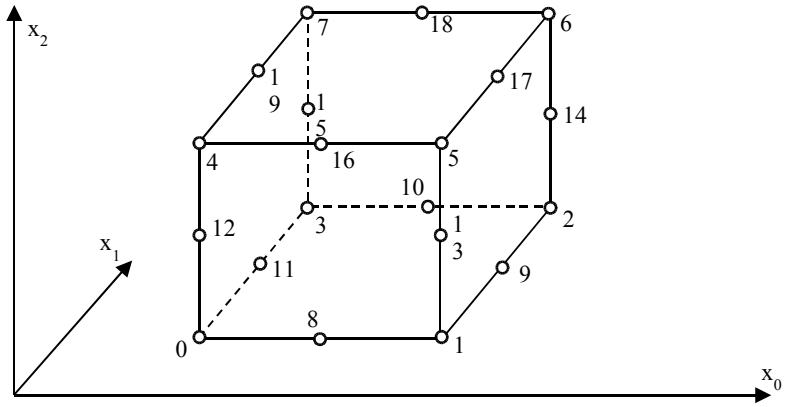

Fig. 2 : 20 Node Serendipity Brick Element

In a vicinity of a contact plane, the brick elements must be distorted considerably from a rectangular shape to adapt to the shape of the contact plane. This leads to errors in the stress distribution which is calculated with the distorted brick elements. This paper investigates the use of the eighteen node wedge elements shown in Fig. 3 for the analysis of arch dams and their abutment.

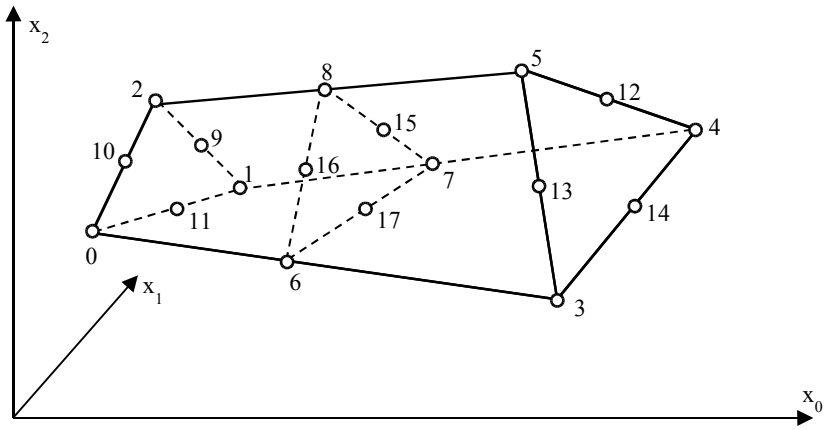

Fig. 3 : 18 Node Wedge Element

The wedge elements are oriented so that their triangular faces lie in an upstream or downstream surface of the arch dam. The triangulations of the upstream and downstream faces of the dam are readily adapted to the curve of the contact plane. If the edges of the wedge elements are choosen to be straight, complete quadratic polynomials can be used for the displacement interpolation in the wedges, leading to a linear stress variation in the global coordinate system. The accuracy of the wedges does not deteriorate in the vicinity of the contact plane.

In order to evaluate the relative accuracy of the two element types in the vicinity of the contact plane between materials of different stiffness, a testbed has been developed. It consists of the rectangular straight cantilever beam shown in Fig. 4 with a contact plane, whose location in the beam can be varied. The contact plane subdivides the beam into two zones with different linear elastic isotropic material properties.

Fig. 4 : Surface of the Testbed

An automatic finite element generator is implemented for the testbed, which can create both brick and wedge grids. The free end of the cantilever is loaded with a distributed surface load, whose components can be specified at the four corners of the end surface. The testbed is used to present isolines of the global components of displacement and stress as well as the principal stresses and their directions on the sections, horizons and faces of the beam.

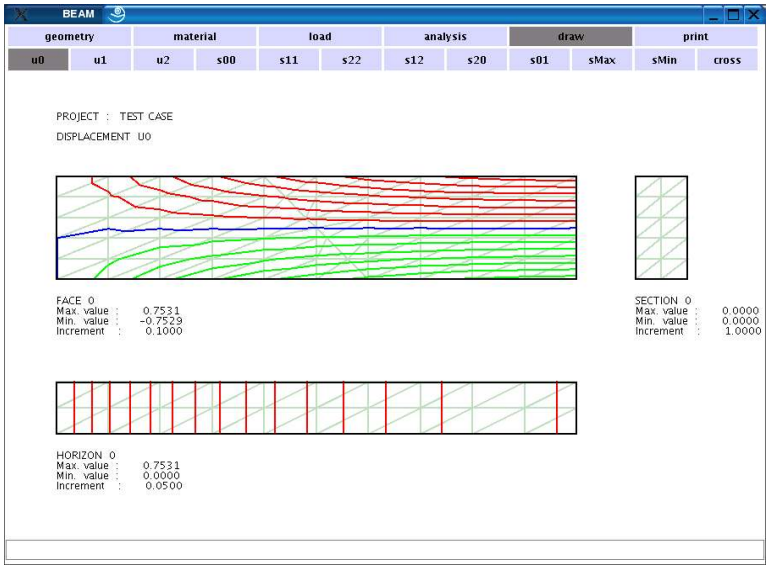

Fig. 5 : Presentation of Isolines

In addition, the components of stress in the local coordinate system of the contact plane as well as the principal stresses and their directions can be presented for points lying just above the contact plane (upper contact plane) and points lying just below the contact plane (lower contact plane), as shown in Fig.6.

Fig. 6 : Contact Plane Representation

2 Comparison of the element types for homogeneous beams

The performance of the brick and wedge elements is compared for a beam with length 10.0, height 2.0, width 1.0, elastic modulus 1000.0 and Poisson ratio 0.0, subjected to a uniformly distributed load 10.0 acting in direction x_1 at the free end of the cantilever. Beam theory neglecting shear deformation predicts a maximum deflection 5.0 and a maximum bending stress 150.0 .

number of			brick grid			wedge grid		
sections	horizons	faces	variables	u	σ	variables	u	σ
6	6	3	1080	5,1164	150,86	1815	5,1108	148,62
		5	1872	5,1164	150,86	3267	5,1108	148,62
6	3	3	513	5,1146	149,80	825	5,1072	147,65
	4		702	5,1159	150,45	1155	5,1098	148,31
	8		1458	5,1165	150,98	2475	5,1111	148,69
	12		2214	5,1166	151,06	3795	5,1111	148,72
3	6	3	513	5,0028	135,93	825	4,9347	127,55
4			702	5,0908	145,49	1155	5,0654	140,40
5			891	5,1102	149,06	1485	5,0992	145,82
6			1080	5,1164	150,86	1815	5,1108	148,62
8			1458	5,1203	152,72	2475	5,1182	151,43
12			2214	5,1221	154,44	3795	5,1213	153,86
16			2970	5,1227	155,34	5115	5,1221	155,07
20			3726	5,1230	155,93	6435	5,1225	155,81
24	10	3	7614	5,1232	157,32	13395	5,1229	157,07
28	16		14388	5,1233	158,27	25575	5,1231	157,88
41	21		27855	5,1235	159,47	49815	5,1233	159,18
51	25		41391	5,1236	160,11	74235	5,1234	159,85

Table 1 : Influence of grid size on a homogeneous beam without contact plane.

The influence of the number of sections, horizons and faces on the maximum displacement and stress in a homogeneous beam is compared in Table 1 for brick and wedge grids. The finest grid with 51*25*3 (sections*horizons*faces) leads to nearly equal results with a maximum deflection

5.1236 or 5.1234 and a maximum stress 160.11 or 159.85 . A 6*6*3 grid leads to displacement errors of 0.14 and 0.25% for brick and wedge grids, and stress errors of 5.8 and 7.2%, as compared to the finest grid. For a 12*6*3 grid, the corresponding errors are 0.029 and 0.045% in the displacement, and 3.5 and 3.9% in the stress. The increase over the bending stress of beam theory is due to stress concentrations at the top and bottom fibres at the support, which are amplified as the grid size decreases.

Consider a beam with a contact plane running from (x_0 , x_1) = (4.0 , 0.0) to (x_0 , x_1) = (6.0 , 2.0). Fig. 7 schematically shows the brick grid and Fig. 8 the wedge grid near the contact plane. If the beam remains homogeneous, the contact plane should not influence the behaviour. The influence of the contact plane on the results for different sizes is shown in Table 2. The trends are comparable to Table 1.

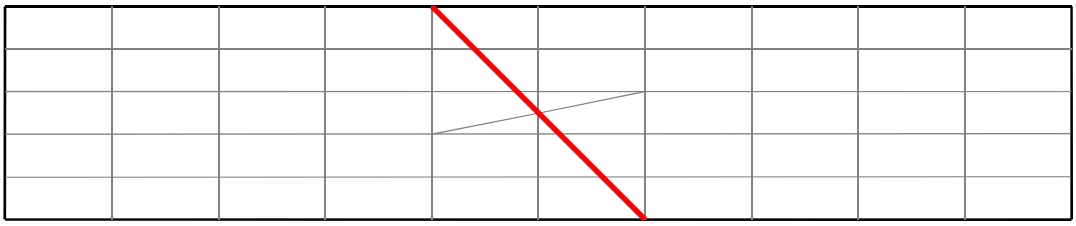

Fig. 7 : Brick grid with contact plane.

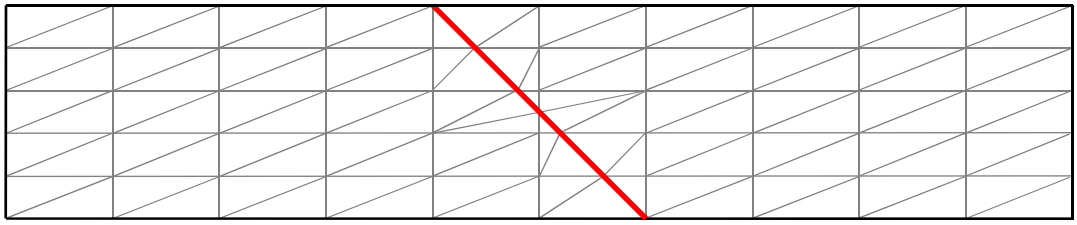

Fig. 8 : Wedge grid with contact plane.

number of			brick grid			wedge grid		
sections	horizons	faces	variables	u	σ	variables	u	σ
6	6	3	1221	5,1164	150,85	2055	5,1122	148,62
		5	2115	5,1164	150,85	3699	5,1122	148,62
6	3	3	555	5,1105	149,82	885	5,1087	147,66
	4		777	5,1149	150,46	1275	5,1113	148,31
	8		1665	5,1167	150,97	2835	5,1123	148,69
	12		2553	5,1169	151,04	4395	5,1124	148,72
3	6	3	753	5,0047	135,63	1215	4,9568	128,43
4			891	5,0968	145,67	1485	5,0792	140,41
5			1131	5,1101	149,18	1875	5,1018	145,88
6			1221	5,1164	150,85	2055	5,1122	148,62
8			1749	5,1201	152,71	2925	5,1185	151,43
12			2505	5,1219	154,44	4245	5,1213	153,86
16			3213	5,1225	155,34	5475	5,1221	155,07
20			4119	5,1228	155,94	7005	5,1225	155,81
24	10	3	8139	5,1231	157,32	14205	5,1229	157,07
28	16		15063	5,1233	158,27	26625	5,1231	157,88
41	21		28623	5,1235	159,47	51015	5,1233	159,18
51	25		42243	5,1235	160,11	75555	5,1234	159,85

Table 2 : Influence of grid size on a homogeneous beam with contact plane.

3 Comparison of shear stresses in the homogeneous beam

Tables 1 and 2 give the impression that the brick elements lead to higher accuracy than the wedge elements. The isolines of shear stress in Fig. 9 and 10 show, however, that the wedge grid remains accurate in the vicinity of the contact plane, whereas the shear stress isolines for the brick grid are disturbed considerably by the contact plane.

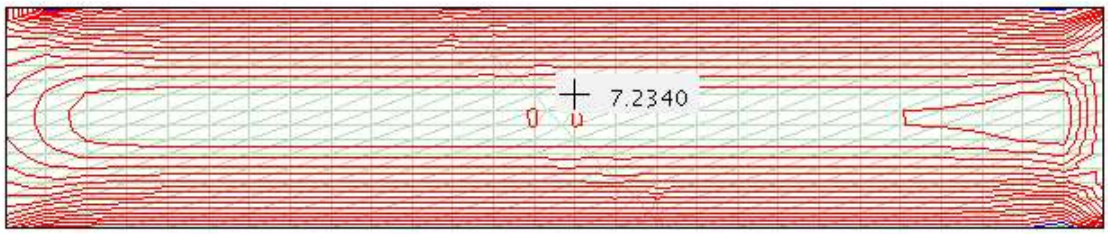

FACE 0
Max. value : 7.9199
Min. value : -0.7405
Increment : 0.5000

Fig. 9 : Shear Stress in face 0 : homogeneous beam with contact plane : wedge grid 28*16*3.

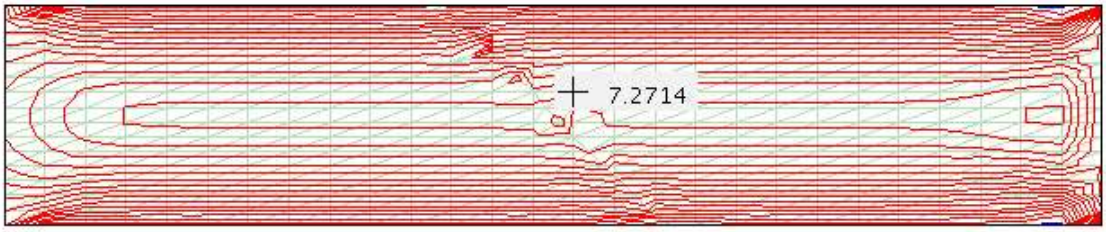

FACE 0
Max. value : 8.1421
Min. value : -0.2572
Increment : 0.5000

Fig. 10 : Shear stress in face 0 : homogeneous beam with contact plane : brick grid 28*16*3.

The error in the shear stress in the vicinity of the contact plane of the homogeneous beam composed of brick elements becomes smaller with Poisson ratio 0.1 as shown in Fig. 11 and with Poisson ratio 0.3 as shown in Fig. 12.

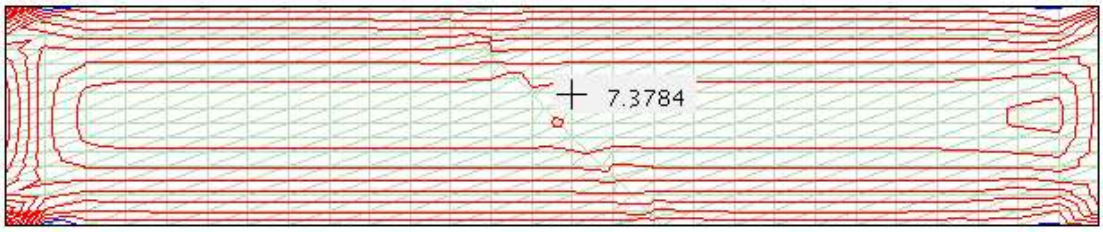

FACE 0
Max. value : 13.3840
Min. value : -1.5004
Increment : 1.0000

Fig. 11 : Shear stress in face 0 : homogeneous beam with contact plane : Poisson ratio = 0.1 : brick grid 28*16*3

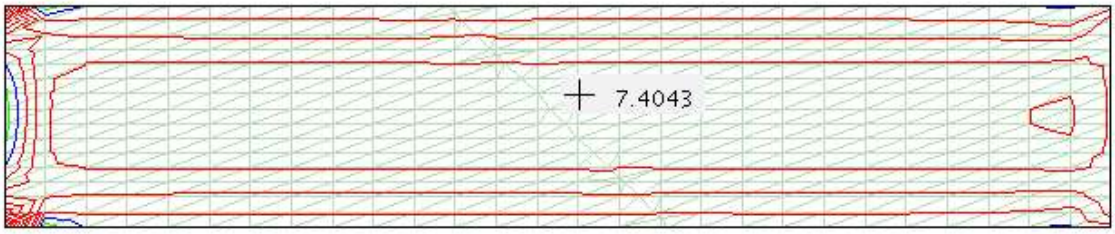

FACE 0
Max. value : 20.8492
Min. value : -3.3472
Increment : 2.0000

Fig. 12 : Shear stress in face 0 : homogeneous beam with contact plane : Poisson ratio = 0.3 : brick grid 28*16*3

4 Influence of heterogeneous material properties

Let the modulus of elasticity be E_1 and E_2 in the left and right zones of the beam. Figures 13 to 15 show the effect of the ratio E_1/E_2 on the distribution of the bending stress in the vicinity of the contact plane. As E_1/E_2 increases, the stress concentration at the upper end of the contact plane increases as expected.

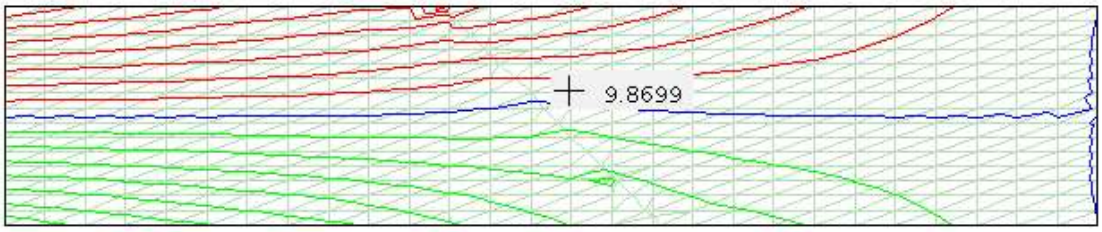

FACE 0
Max. value : 158.2721
Min. value : -158.2685
Increment : 20.0000

Fig. 13 : Normal stress in face 0 : $E_1/E_2 = 0.5$: v = 0.0 : brick grid 28*16*3

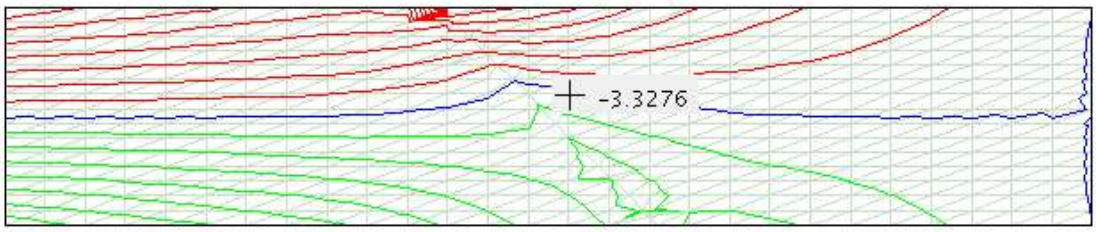

FACE 0
Max. value : 238.0755
Min. value : -158.2665
Increment : 20.0000

Fig. 14 : Normal stress in face 0 : $E_1/E_2 = 0.2$: v = 0.0 : brick grid 28*16*3

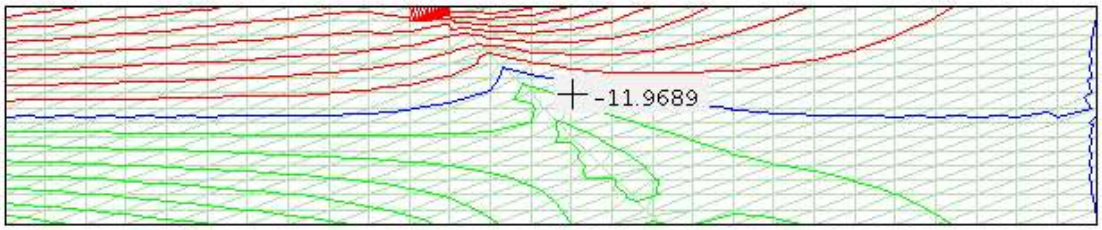

FACE 0
Max. value : 301.9141
Min. value : -158.2652
Increment : 20.0000

Fig. 15 : Normal stress in face 0 : E_1/E_2= 0.1 : v = 0.0 : brick grid 28*16*3

Figures 16 to 18 show the effect of the ratio E_1/E_2 on the distribution of the shear stress in the vicinity of the contact plane. The shear stress increases with the ratio E_1/E_2, as expected. The distortion of the brick element leads to significant distortions in the isolines for the shear stress.

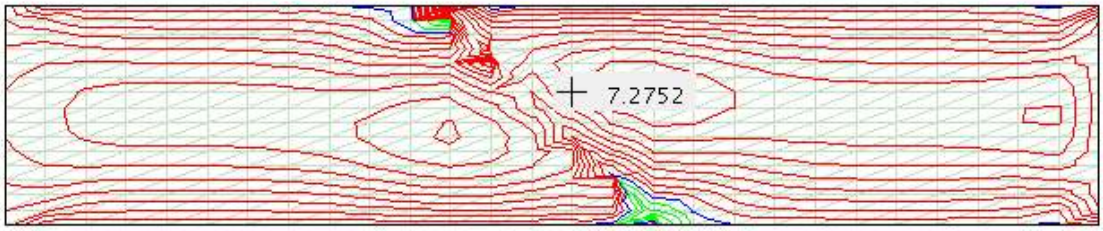

FACE 0
Max. value : 12.1886
Min. value : -4.3197
Increment : 1.0000

Fig. 16 : Shear stress in face 0 : E_1/E_2 = 0.5 : v = 0.0 : brick grid 28*16*3

FACE 0
Max. value : 42.3551
Min. value : -11.2076
Increment : 5.0000

Fig. 17 : Shear stress in face 0 : E_1/E_2 = 0.2 : v = 0.0 : brick grid 28*16*3

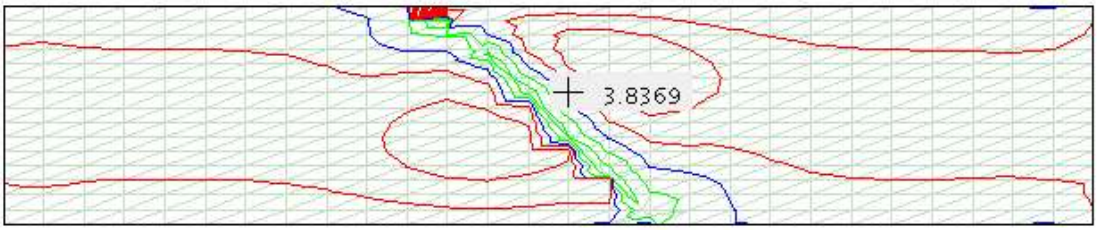

FACE 0
Max. value : 70.2227
Min. value : -16.1653
Increment : 5.0000

Fig. 18 : Shear stress in face 0 : $E_1/E_2 = 0.1$: $v = 0.0$: brick grid 28*16*3

Figures 19 and 20 show the stress component parallel to the contact plane and normal to axis x_2 for $E_1/E_2 = 0.2$ and Poisson ratio 0.0 . The ratio 0.2182 of the stresses above and below the contact plane approximately equals the ratio E_1/E_2 as expected.

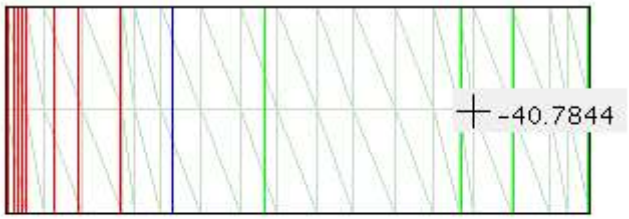

UPPER CONTACT PLANE
Max. value : 167.4893
Min. value : -40.7844
Increment : 20.0000

Fig. 19 : Stress in the upper contact plane : $E_1/E_2 = 0.2$: $v = 0.0$: brick grid 28*16*3

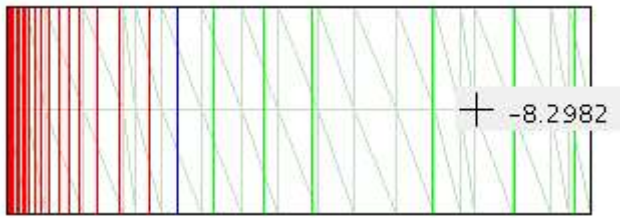

LOWER CONTACT PLANE
Max. value : 34.0370
Min. value : -8.3110
Increment : 2.0000

Fig. 20 : Stress in the lower contact plane : $E_1/E_2 = 0.2$: $v = 0.0$: brick grid 28*16*3

5 Bending about the vertical axis x_2

If the beam is loaded in the transverse direction x_2, the quality of the bending stresses which are determined with the wedge and brick elements are comparable to those described in section 2 for bending under load in direction x_1. Fig. 21 and 22 show the shear stresses in face 0 and horizon 0 under transverse load for the two element types. The theoretical shear stress in face 0 is zero. The solution with wedge elements shows low shear stresses except in the vicinity of the support. The solution with brick elements shows significant shear stress at the contact plane.

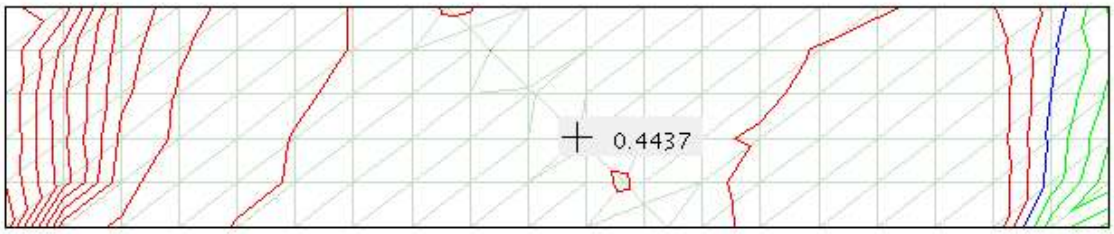

FACE 0
Max. value : 5.7609
Min. value : -1.8417
Increment : 0.5000

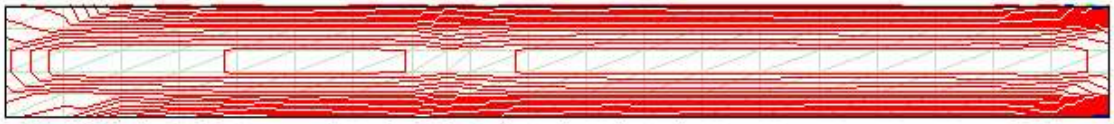

HORIZON 0
Max. value : 8.4000
Min. value : -1.0675
Increment : 0.5000

Fig. 21 : Shear stress in face 0 and horizon 0 : bending force = 5.0 : wedge grid 20*6*6

FACE 0
Max. value : 22.2401
Min. value : -6.6787
Increment : 2.0000

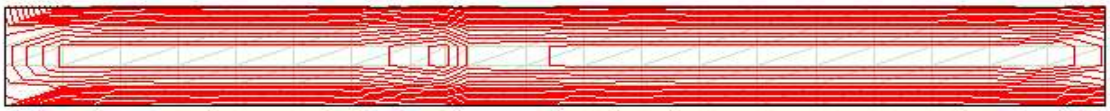

HORIZON 0
Max. value : 9.1877
Min. value : 0.4194
Increment : 0.5000

Fig. 22 : Shear stress in face 0 and horizon 0 : bending force = 5.0 : brick grid 20*6*6

6 Grid generator

The main component of the testbed is a generator for wedge element and brick element grids for cantilever beams with different dimensions, loadings and contact planes. In analogy to the arch dam, only the elementation of the beam near the contact plane deviates from the pattern prescribed by the horizontal and vertical planes of the joints of the dam.

The generators are pattern-driven (Pahl and Mironov 2004). Fig. 23 shows a typical pattern for the wedge grid. Fig. 24 shows a typical pattern for the brick grid.

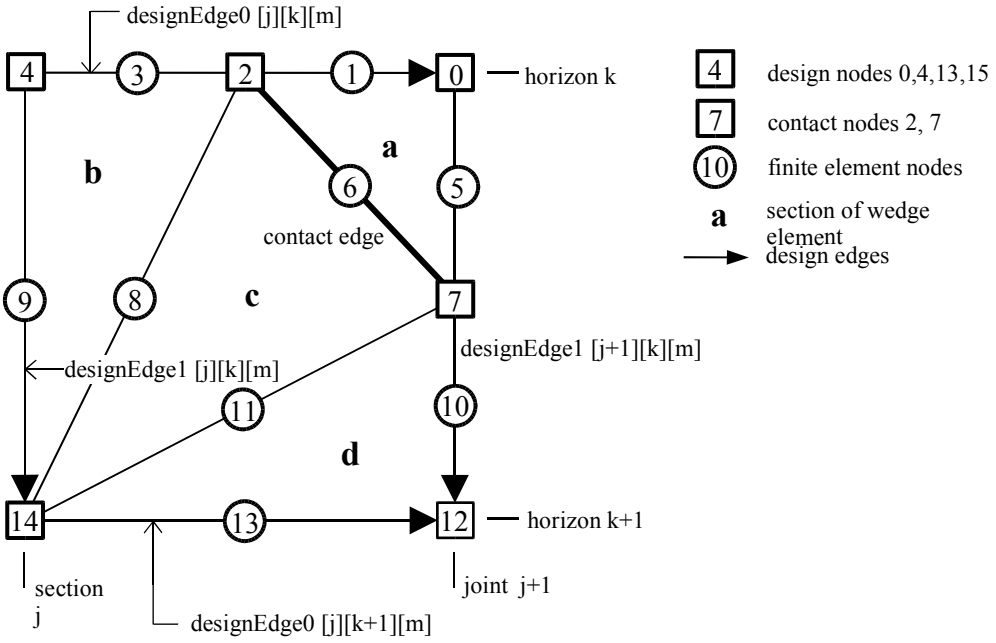

Fig. 23 : Typical pattern for the wedge grid

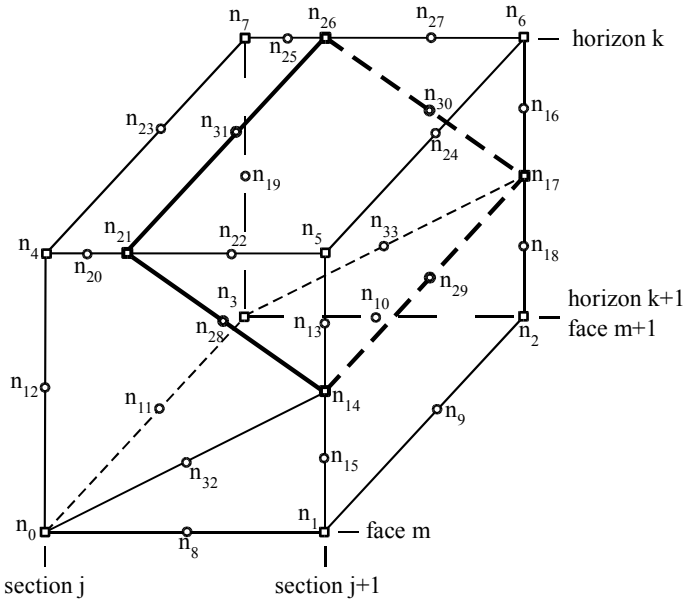

Fig. 24 : Typical pattern for the brick grid

7 Conclusions.

The investigation shows that in a homogeneous beam, the two element types which both have C_0-compatibility converge to the same displacements and stresses. In a rectangular grid with a given number of sections, horizons and faces, the brick is slightly more accurate than the wedge. The number of variables in a brick grid is approximately 60% of that in a wedge grid. This influences the numerical effort for the solution of the system equations.

If the element grid is deformed near a contact plane, the accuracy of the brick grid deteriorates whereas that of the wedge grid does not change significantly. This effect is enhanced if the ratio of the moduli of elasticity on the two sides of the contact plane is increased. Additional factors of influence such as the aspect ratio of the beam and the location and inclination of the contact plane remain to be investigated.

8 References

Bathe, K.-J. (1986). Finite-Elemente-Methoden. Springer-Verlag. ISBN 3-540-15602-X. p. 223, 315, 321 .

Pahl, P.J. and Mironov, V.N. (2004). Generator for a Beam with Contact Plane. Internal Report. FG Theoretische Methoden der Bau- und Verkehrstechnik. Technische Universität Berlin. Germany.

Zienkiewicz, O.C. (1977). The Finite Element Method, 3. Edition. McGraw Hill. ISBN 0-07-084072-5. p. 218 .